2. F. Liu, I. Turner, and M. Bialkowski, A finite-difference time-domain simulation of power density distribution in a dielectric loaded microwave cavity, J Microwave Power Electromagn Energy 29 (1994), 138–149.
3. S. Hanafusa, T. Iwasaki, and N. Nishimura, Electromagnetic field analysis of a microwave oven by the FD-TD method: A consideration on steady state analysis, IEEE Antennas Propagat Soc Int Symp, Seattle, WA, 1994, vol. 3, pp 1806–1809.
4. L. Ma, D. Paul, N. Pothecary, C. Railton, J. Bows, L. Barratt, J. Mullin, and D. Simons, Experimental validation of a combined electromagnetic and thermal FDTD model of a microwave heating process, IEEE Trans Microwave Theory Tech 43 (1995), 2565–2572.
5. A. Taflove and S.C. Hagness, Computational electrodynamics—the finite-difference time-domain method, 2nd ed., Artech House, Norwood, MA, 2000.
6. R.E. Collin, Foundations for microwave engineering, McGraw Hill, New York, 1966.
7. A.C. Metaxas and R.J. Meredith, Industrial microwave heating, IEE Power Engineering Series, Peter Peregrinus Ltd., London, 1993.
8. G. Mur, Absorbing boundary conditions for the finite-difference approximations of the time domain electromagnetic field equations, IEEE Trans Electromagn Compat 23 (1981), 377–382.

A BROADBAND PRINTED BOW-TIE ANTENNA WITH A SIMPLIFIED BALANCED FEED

Guiping Zheng, Ahmed A. Kishk, Allen W. Glisson, and Alexander B. Yakovlev
Department of Electrical Engineering
Center for Applied Electromagnetic Systems Research (CAESR)
University of Mississippi
University, MS 38677-1848

Received 5 June 2005

ABSTRACT: *A broadband printed bow-tie antenna with a simplified balanced feeding network and modified tapering is presented. Microstrip and parallel-strip transmission lines printed on the substrate with high dielectric permittivity realize the proposed feeding network. The ground-plane transition between the microstrip line and the parallel-strip line is exponentially tapered so as to reduce the reflection losses and produce a balanced feed for the antenna. This printed bow-tie antenna achieves a 68% measured bandwidth and a stable radiation pattern within the X-band. Commercial FEM software is used for optimization of the bow-tie antenna and the simulation results agree very well with the experiment.* © 2005 Wiley Periodicals, Inc. Microwave Opt Technol Lett 47: 534–536, 2005; Published online in Wiley InterScience (www.interscience.wiley.com). DOI 10.1002/mop.21221

Key words: *broadband antenna; bow-tie antenna; feeding network; microstrip line*

1. INTRODUCTION

New configurations of a simplified feeding network for a printed dipole antenna have been recently presented in [1, 2]. In the proposed designs, the feeding network is realized by a microstrip line (implemented on a grounded dielectric slab) coupled to a parallel-strip transmission line. The upper part of the feed/antenna structure consists of a microstrip line connected to one of the parallel lines and one arm of the printed dipole antenna. The lower part consists of a truncated ground plane directly connected to the other parallel line, which is transitioned to the second arm of the dipole antenna (printed on the same surface of substrate). The truncated ground plane acts as a reflector, resulting in a high front-to-back ratio radiation pattern. In [3], a similar feeding-network configuration was proposed for a printed bow-tie antenna. However, in this design the truncated ground plane has a different role and does not act as a reflector, as in the designs presented in [1, 2]. The feeding networks presented in [4–10] achieve a balanced antenna current in a very narrow band. In addition, these feeding networks are structurally complicated and include additional elements, such as a T-junction, power divider, microstrip-line discontinuity taper, and microstrip-to-coplanar stripline (CPS) balun. In the proposed simplified feeding network used in the modified printed Yagi antenna designs [1, 2], reflection losses are reduced significantly and the efficiency of the network is greatly improved. However, these designs have a relatively narrow bandwidth compared to those in [4, 5] because the two arms of the dipole antenna reside on the opposite sides of substrate with high dielectric permittivity.

In this paper, we propose a new design based on the simplified feeding network in conjunction with a broadband printed bow-tie antenna [11]. The new design features broadband operation and a stable broad main-beam radiation pattern in the X-band.

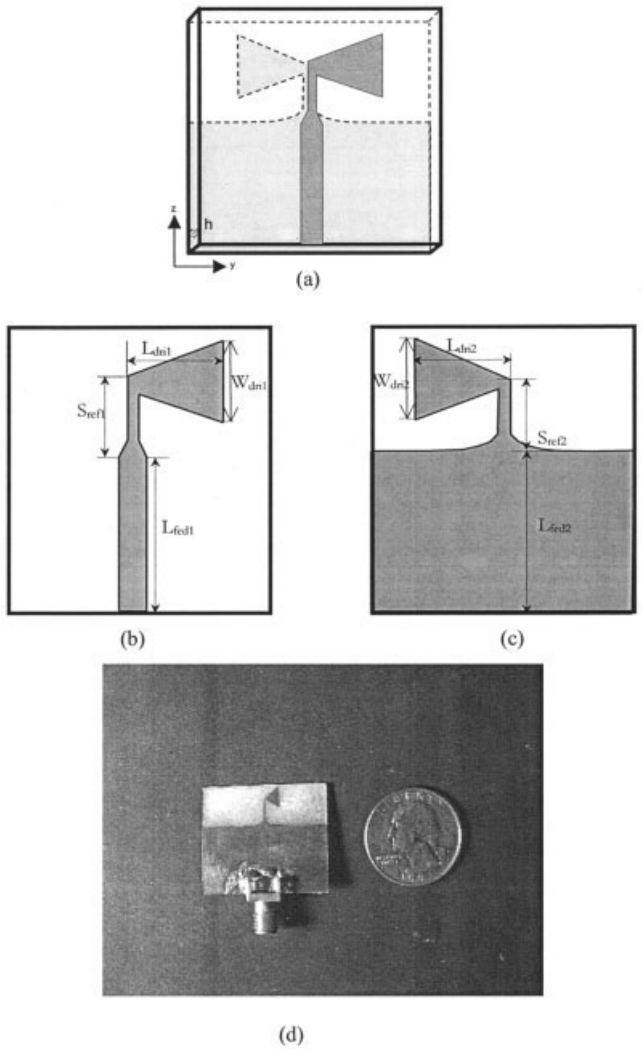

Figure 1 Geometry of printed bow-tie antenna with a simplified feeding network: (a) 3D schematic view; (b) top layer; (c) bottom layer; and (d) photograph of the fabricated antenna

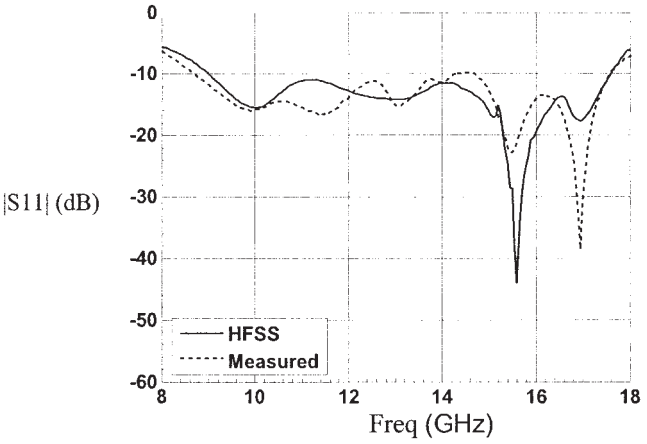

Figure 2 Computed and measured reflection coefficients of the printed bow-tie antenna

2. SIMPLIFIED FEEDING NETWORK CONFIGURATION

Figure 1 shows the geometry of broadband printed bow-tie antenna with a simplified feeding network. The feed/antenna structure is printed on Rogers RT/6010LM substrate of thickness 0.64 mm with a high dielectric permittivity of 10.2. The resonance length of the bow-tie antenna at 10 GHz is calculated by

$$L_{bow\text{-}tie} = \frac{\lambda_g}{2} \cdot \frac{c}{2\lambda_0\sqrt{\varepsilon_{eff}}}, \tag{1}$$

where c is the velocity of light in free space and ε_{eff} is the approximate effective dielectric permittivity obtained by averaging the permittivities of free space and dielectric substrate. By carefully adjusting the length and flare angle of the bow-tie antenna along with the feed parameters, an optimized antenna design with broad matching bandwidth can be achieved.

The feeding structure used in the design of the printed bow-tie antenna is similar to that proposed in [1, 2] in the design of the modified printed Yagi antenna. Here, we modified the feeding network by introducing an exponential taper between the microstrip line and the parallel-strip line so as to reduce the reflection losses and produce a balanced feed for the bow-tie antenna. The microstrip line, designed to a 50Ω characteristic impedance, is connected to a 50Ω coaxial connector (used with the 50Ω coaxial cable of the network analyzer for the measurements). The parallel-strip transmission line is designed to an 80Ω characteristic impedance.

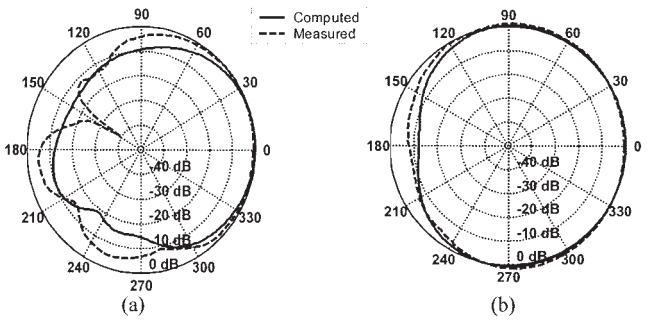

Figure 3 Computed and measured radiation patterns for the printed bow-tie antenna at 10 GHz: (a) E-plane; (b) H-plane

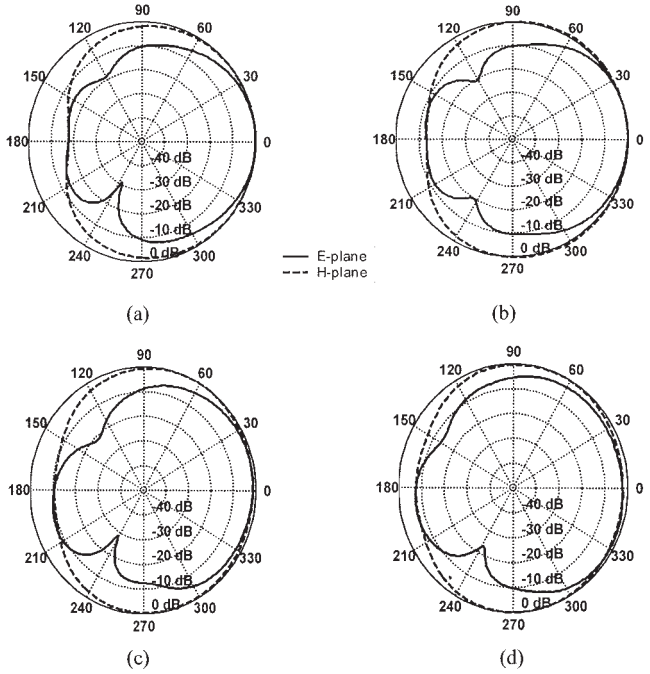

Figure 4 Computed radiation patterns for the printed bow-tie antenna in the E-plane and H-plane: (a) 9 GHz; (b) 11 GHz; (c) 12 GHz; (d) 13 GHz

The following dimensions have been used in the design of the printed bow-tie antenna and its feeding network (units in mm): $L_{dri1} = L_{dri2} = 3.53$, $W_{dri1} = W_{dri2} = 5.3$, $L_{fed1} = L_{fed2} = 16$, and $S_{ref1} = S_{ref2} = 6.5$. The total area of the substrate is approximately $\lambda_0 \times \lambda_0$ at 10 GHz. The proposed antenna was built and tested, and the measured data were obtained using an HP 8510C vector network analyzer. The simulated and measured reflection coefficients are shown in Figure 2. The difference between the simulated and measured results is mainly due to change in the substrate thickness, which occurred in the fabrication process of the bow-tie antenna and its feeding network by using a milling machine. The simulated and measured radiation patterns in the E-plane and H-plane at 10 GHz are compared in Figure 3. Figure 4 shows the computed radiation patterns in the frequency range from 9 to 13 GHz. The results show that the matching bandwidth is more than 65%. The radiation patterns are computed for different frequencies, indicating a wide beamwidth within the matching band. The front-to-back radiation level is about 10 dB. Increasing the ground-plane size can increase the front-to-back ratio level. The radiation patterns show symmetry around the broadside direction, indicating a well-balanced condition within the matching bandwidth (except for a small asymmetry at 13 GHz).

3. CONCLUSION

A broadband bow-tie antenna with a simplified feeding network printed on substrate with high dielectric permittivity has been investigated. The antenna achieved a matching bandwidth of 68% with a stable broad main beam in the radiation pattern within the X-band. The front-to-back radiation level is approximately 10 dB, which can be increased by increasing the ground-plane size. The small size of antenna and broad main beam of its radiation pattern indicate that it is a good candidate for phased antenna arrays.

REFERENCES

1. G. Zheng, A.A. Kishk, A.B. Yakovlev, and A.W. Glisson, Simplified feeding for a modified printed Yagi antenna, IEEE AP-S Int Symp Dig 3 (2003), 934–937.

2. G. Zheng, A.A. Kishk, A.B. Yakovlev, and A.W. Glisson, Simplified feed for a modified printed Yagi antenna, Electron Lett 40 (2004), 464–465.
3. K. Kiminami, A. Hirata, and T. Shiozawa, Double-sided printed bow-tie antenna for UWB Communications, IEEE Antennas Wireless Propagat Lett 3 (2004), 152–153.
4. Y. Qian, W.R. Deal, N. Kaneda, and T. Itoh, Microstrip-fed quasi-Yagi antenna with broadband characteristics, Electron Lett 34 (1998), 2194–2196.
5. Y. Qian, W.R. Deal, N. Kaneda, and T. Itoh, A uniplanar quasi-Yagi antenna with wide bandwidth and low mutual coupling characteristics, IEEE AP-S Int Symp Dig 2 (1999), 924–927.
6. W.R. Deal, N. Kaneda, J. Sor, Y. Qian, and T. Itoh, A new quasi-Yagi antenna for planar active antenna arrays, IEEE Trans Microwave Theory Tech 48 (2000), 910–918.
7. H.J. Song and M.E. Bialkowski, Investigations into the operation of a microstrip-fed uniplanar quasi-Yagi antenna, IEEE AP-S Int Symp Dig 3 (2000), 1436–1439.
8. C. Ha, Y. Qian, and T. Itoh, A modified quasi-Yagi planar antenna with wideband characteristics in C-band, IEEE AP-S Int Symp 3 (2001), 154–157.
9. N. Kaneda, W.R. Deal, Y. Qian, R. Waterhouse, and T. Itoh, A broadband planar quasi-Yagi antenna, IEEE Trans Antennas Propagat 50 (2002), 1158–1160.
10. A.A. Eldek, A.Z. Elsherbeni, and C.E. Smith, Wideband microstrip-fed printed bow-tie antenna for phased-array systems, Microwave Opt Technol Lett 43 (2004), 123–126.
11. G. Zheng, A.A. Kishk, A.B. Yakovlev, and A.W. Glisson, A broadband printed bow-tie antenna with a simplified feed, IEEE AP-S Int Symp Dig 4 (2004), 4024–4027.

MICROWAVE IMAGING OF CONCEALED METAL OBJECTS USING A NOVEL INDIRECT HOLOGRAPHIC METHOD

M. Elsdon, D. Smith, M. Leach, and S. Foti
School of Engineering and Technology
Northumbria University
Newcastle-Upon-Tyne, NE1 8ST, U. K.

Received 3 June 2005

ABSTRACT: *A novel, inexpensive technique for the detection of concealed metal objects is presented and discussed. It is shown that an indirect holographic method, usually employed at optical frequencies, can be adapted to image objects at microwave frequencies. The practical results successfully demonstrate that this technique can be used to determine the location and shape of the concealed object.* © 2005 Wiley Periodicals, Inc. Microwave Opt Technol Lett 47: 536–537, 2005; Published online in Wiley InterScience (www.interscience.wiley.com). DOI 10.1002/mop.21222

Key words: *microwave imaging; concealed weapons detection; holography*

1. INTRODUCTION

The ability of microwaves to image concealed objects using a wide variety of radar techniques is well documented [1–3]. One such technique is that of direct holography, which has been primarily developed for the determination of antenna radiation characteristics and the imaging of antenna fields [4, 5]. In these techniques, the complex fields of the antenna are measured over an aperture close to the antenna using a vector network analyzer. These results can then be mathematically transformed in order to produce the field distribution over the antenna. One major disadvantage of this technique is its inefficiency in terms of time. Moreover, as such a system requires the use of a vector network analyzer, the cost is dramatically increased.

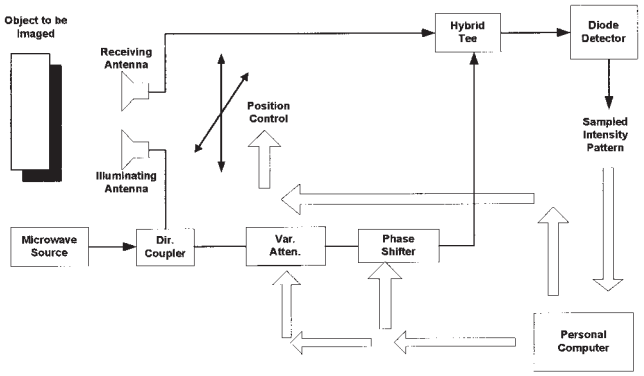

Figure 1 Experimental arrangement for indirect microwave holographic imaging

A simpler indirect holographic technique which enables the complex aperture field to be reconstructed from a single scalar-intensity pattern has recently been reported [6]. In this paper, it is shown how this technique can be extended to image concealed weapons in a simple and inexpensive manner.

2. INDIRECT HOLOGRAPHY

Indirect holographic imaging consists of two stages. The first stage is the recording of a sampled intensity pattern, while the second stage is concerned with image reconstruction. An outline of the experimental system used to achieve this is shown in Figure 1.

The recording of a sampled intensity pattern, $I(x, y)$, is formed by combining the scattered signal from the object, $E(x, y)$, with a reference signal, $R(x, y)$, as follows:

$$I(x, y) = |E(x, y) + R(x, y)|^2 = |E(x, y)|^2 + |R(x, y)|^2 + E(x, y)\,R^*(x, y) + E^*(x, y)\,R(x, y). \quad (1)$$

Previously, for antenna measurements, the object to be imaged was an active source of microwave radiation. However, for imaging of passive objects, the object must be illuminated with a source of microwave radiation.

At optical frequencies, image reconstruction is performed by re-illuminating the hologram with the original reference signal. In order to obtain an unobscured image of the original object, this reference signal must be introduced at an offset angle [7]. The adoption of a similar technique at microwave frequencies has proved difficult due to the practical problem associated with providing an offset reference wave. To overcome this, in the proposed

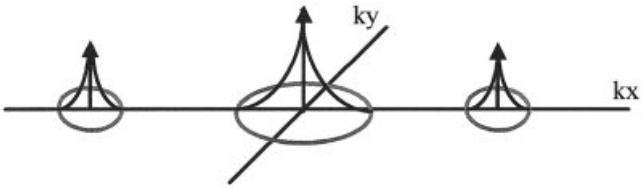

Figure 2 Spectral representation of an off-axis hologram